© 2018. Published by The Company of Biologists Ltd | Journal of Cell Science (2018) 131, jcs215251. doi:10.1242/jcs.215251

RESEARCH ARTICLE

Balanced Rac1 activity controls formation and maintenance of neuromuscular acetylcholine receptor clusters

Yanyang Bai[1,*], Daji Guo[1], Xiaoyu Sun[1], Genyun Tang[2], Tailin Liao[3], Yinghui Peng[1], Junyu Xu[3] and Lei Shi[1,‡]

ABSTRACT

Rac1, an important Rho GTPase that regulates the actin cytoskeleton, has long been suggested to participate in acetylcholine receptor (AChR) clustering at the postsynaptic neuromuscular junction. However, how Rac1 is regulated and how it influences AChR clusters have remained unexplored. This study shows that breaking the balance of Rac1 regulation, by either increasing or decreasing its activity, led to impaired formation and maintenance of AChR clusters. By manipulating Rac1 activity at different stages of AChR clustering in cultured myotubes, we show that Rac1 activation was required for the initial formation of AChR clusters, but its persistent activation led to AChR destabilization, and uncontrolled hyperactivation of Rac1 even caused excessive myotube fusion. Both AChR dispersal and myotube fusion induced by Rac1 were dependent on its downstream effector Pak1. Two Rac1 GAPs and six Rac1 GEFs were screened and found to be important for normal AChR clustering. This study reveals that, although general Rac1 activity remains at low levels during terminal differentiation of myotubes and AChR cluster maintenance, tightly regulated Rac1 activity controls normal AChR clustering.

KEY WORDS: Neuromuscular junction, Acetylcholine receptor, Agrin, Rho GTPase, Rac1, Actin

INTRODUCTION

The formation, dispersal and maintenance of acetylcholine receptors (AChRs) at the neuromuscular junction (NMJ) require a highly dynamic control of local cytoskeleton (Sanes and Lichtman, 1999, 2001; Shi et al., 2012; Wu et al., 2010). In general, anchorage of AChR clusters to the cytoskeleton, mediated by a plethora of scaffold proteins, such as rapsyn and the dystrophin–glycoprotein complex, determines the stability of the receptor clusters (Gautam et al., 1995; Gawor and Proszynski, 2017; Jacobson et al., 2001). However, the local cytoskeleton environment, such as actin polymerization/depolymerization, is crucial for the dynamic addition/removal of AChRs at the synaptic sites (Dai et al., 2000; Dobbins et al., 2006). For example, addition and loss of AChRs are both found to occur at the sites of actin polymerization, suggesting that elevated actin dynamics is associated with poor stability or high turnover of AChRs (Basu et al., 2015; Lee et al., 2009; Proszynski et al., 2009).

The Rho family of small GTPases, including RhoA, Rac1 and Cdc42, is one of the main regulators of actin cytoskeleton and is found to have important roles in AChR clustering mediated by agrin, a factor secreted by neurons, which aids postsynaptic organization of neuromuscular junctions and other signals, such as laminin and Wnt (Henriquez et al., 2008; Linnoila et al., 2008; Nizhynska et al., 2007; Weston et al., 2003, 2000). The activity of Rho GTPases are controlled by two classes of regulatory protein, guanine nucleotide exchange factors (GEFs) and GTPase-activating proteins (GAPs), which activate and inactivate Rho GTPases, respectively (Bai et al., 2015; Rossman et al., 2005; Tcherkezian and Lamarche-Vane, 2007). *In vivo* activation of RhoA through the RhoA GEF ephexin1 (Ngef) selectively removes receptors within the AChR clusters, leading to morphological maturation of the clusters (Shi et al., 2010a, b). Rac1 activity has long been suggested to mediate the formation of AChR clusters, but may also participate in the endocytosis of AChRs (Henriquez et al., 2008; Kumari et al., 2008; Weston et al., 2003, 2000). Nonetheless, how Rac1 activity influences AChR clusters *in vivo*, and which GEFs and GAPs are involved in Rac1 regulation during AChR clustering has not been explored.

In our present study, we show that global expression of constitutively active Rac1 in cultured myotubes caused excessive myotube fusion. Interestingly, only transient Rac1 activation was induced following addition of agrin, and both prolonged Rac1 activation as well as Rac1 inhibition impair formation of AChR clusters. Moreover, AChR clusters are smaller and easier to destabilize after Rac1 activation. We further found that the serine/threonine-protein kinase Pak 1 (Pak1) is a major downstream effector mediating the effect of Rac1 on myotube fusion and AChR cluster dispersal. Finally, several Rac1 GEFs and GAPs were identified to be important for normal AChR cluster formation.

RESULTS

Constitutive activation of Rac1 in cultured myotubes leads to abnormal myotube fusion

To study the function of Rac1 in the regulation of AChR clustering, we transfected the mRNAs of Rac1 wild-type (Rac1-WT), constitutively active Rac1 (Rac1-G12V) or dominant-negative Rac1 (Rac1-T17N) in cultured C2C12 myotubes. By using mRNAs, we were able to achieve high transfection efficiency (>90% of the myotubes were transfected) and rapid expression (2 h post transfection; Fig. S1A,B) (Shi et al., 2010a). Surprisingly, myotubes expressing Rac1-G12V fused together extensively, exhibiting more ‘myopatches’ instead of myotubes (Fig. 1A,B). Rac1-Q61L, another constitutively active Rac1 mutant that locks Rac1 at the GTP-bound state by disrupting its GTPase activity,

[1]JNU-HKUST Joint Laboratory for Neuroscience and Innovative Drug Research, College of Pharmacy, Jinan University, Guangzhou 510632, Guangdong, China. [2]Department of Medical Genetics, Hunan Provincial Key Laboratory of Dong Medicine, Hunan University of Medicine, Huaihua 418000, Hunan, China. [3]Department of Neurobiology, Key Laboratory of Medical Neurobiology of Ministry of Health, Zhejiang Province Key Laboratory of Neurobiology, Zhejiang University School of Medicine, Hangzhou 310058, Zhejiang, China.
*Present address: Centre for Gene Editing Brain Disease Models, The Brain Cognition and Brain Disease Institute, Shenzhen Institutes of Advanced Technology, Chinese Academy of Sciences, 1068 Xueyuan Boulevard, Xili, Nanshan, Shenzhen 518055, China.

‡Author for correspondence (sophielshi80@gmail.com)

Y.B., 0000-0002-9923-6843; D.G., 0000-0002-6316-3443; X.S., 0000-0001-7076-5648; G.T., 0000-0001-7936-1594; T.L., 0000-0001-8728-1033; Y.P., 0000-0002-6714-5023; L.S., 0000-0001-8695-3432

Received 17 January 2018; Accepted 2 July 2018

Journal of Cell Science (2018) 131, jcs215251. doi:10.1242/jcs.215251

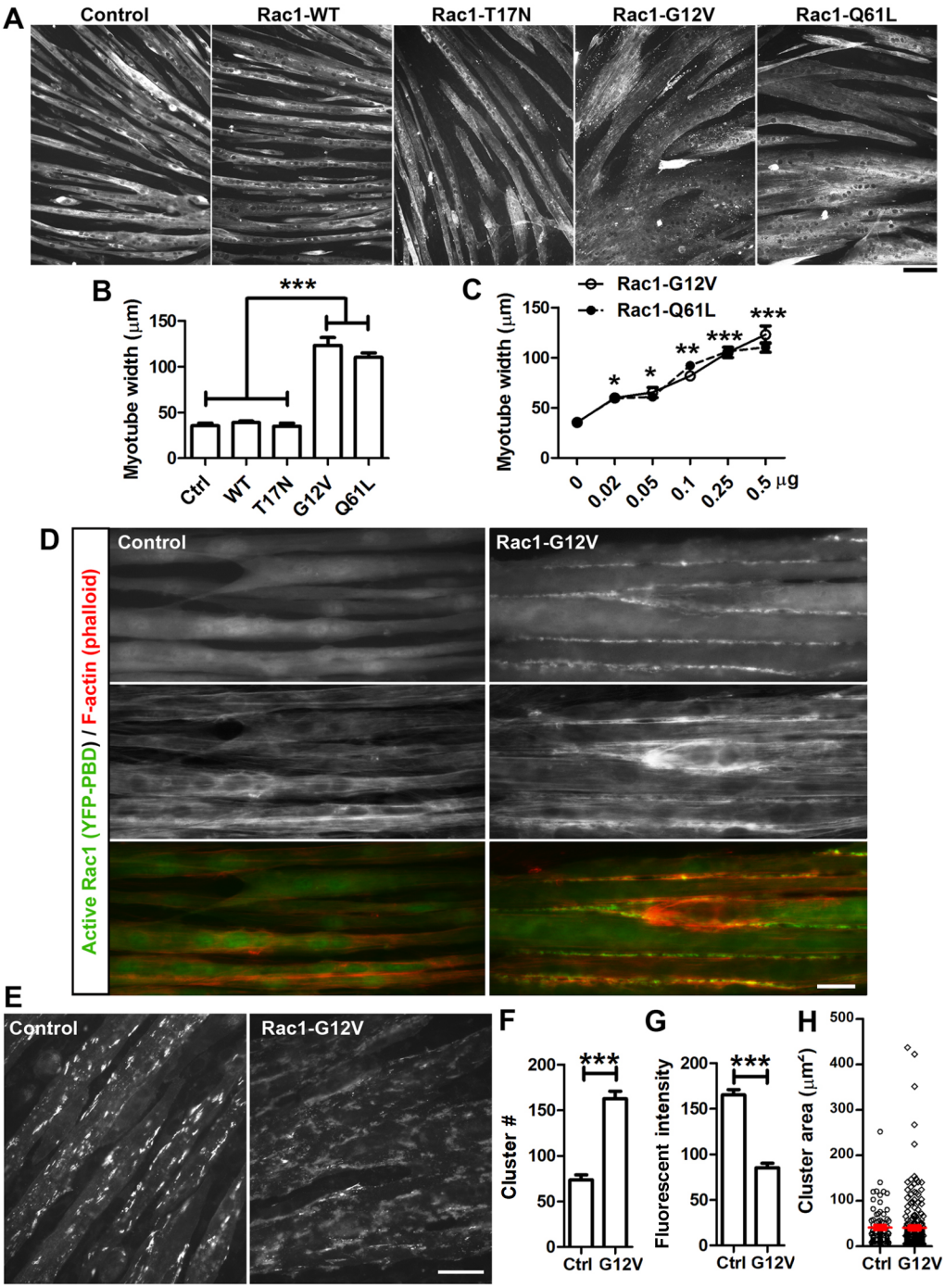

Fig. 1. Hyperactivation of Rac1 in cultured myotubes leads to abnormal myotube fusion. (A) Different Rac1 plasmids were transfected in cultured C2C12 myotubes that had differentiated for 3.5 days. 24 h later, myotubes were stained with anti-myosin heavy chain (MHC) antibody. Scale bar: 100 µm. (B) The width of myotubes was quantified as an indication of myotube fusion. Both constitutively active Rac1 plasmids Rac1-G12V (G12V) and Rac1-Q61L (Q61L) caused severe myotube fusion. ***P<0.001, Rac1-G12V or Rac1-Q61L vs Ctrl, Rac1-WT or Rac1-T17N, one-way ANOVA followed by Bonferroni multiple comparison test. (C) Different amounts of Rac1-G12V or Rac1-Q61L (0.02–0.5 µg) were tested for myotube fusion. *P<0.05, **P<0.01, ***P<0.001, Rac1-G12V or Rac1-Q61L vs Ctrl, one-way ANOVA followed by Bonferroni multiple comparison test. (D) Constitutively active Rac1 colocalized with F-actin and the fusion sites of myotubes. YFP-PBD was transfected together with Rac1-G12V into C2C12 myotubes. F-actin was stained by Rhodamine-phalloidin. Top panels: YFP-PBD signals; middle panels: F-actin signals; bottom panels: Merged signals of YFP-PBD (green) and F-actin (red). Scale bar: 50 µm. (E) Hyperactivation of Rac1 disrupts AChR clustering. Rac1-G12V was transfected into C2C12 myotubes and agrin was added for 8 h. AChR clusters were stained with Alexa Fluor555-conjugated to α-BTX. Scale bar: 50 µm. (F–H) Numbers of AChR clusters (F), fluorescent intensity (G) and size of cluster area (H) were quantified. ***P<0.001, Student's t-test; 10 images were quantified in each experiment. All data shown in this figure are presented as mean ±s.e.m. from at least three independent experiments.

induced myotube fusion similar to that of Rac1-G12V (Fig. 1A,B). Decreasing the amount of Rac1-G12V or Rac1-Q61L mRNA by as much as 25 times (0.02 µg) still induced myotube fusion (Fig. 1C). By contrast, increasing the amount of Rac1-WT mRNA 10 times (5 µg) did not affect the myotube width (Fig. S2), suggesting that there are highly regulated mechanisms for Rac1 inhibition in mature myotubes. To study how constitutive activation of Rac1 affects myotube morphology, we labeled active Rac1 by transfecting mRNA of the Rac1-binding domain (PBD) of Pak1 tagged to that of yellow fluorescent protein (YFP-PBD), a probe that specifically binds to the active GTP-bound form of Rac1 (Hoppe and Swanson, 2004). Filamentous actin (F-actin) was stained with Rhodamine-phalloidin. In control myotubes, we hardly observed signals of active Rac1, and F-actin signals were generally diffuse with higher distribution at the myotube surface (Fig. 1D, left). In Rac1-G12V-transfected myotubes, however, active Rac1 was strongly labeled at the junctional surface of fusing myotubes, where it strongly colocalized with concentrated F-actin (Fig. 1D, right). When agrin was added to induce AChR clustering, the number of clusters found in Rac1-G12V transfected myotubes was increased by more than double (Fig. 1E,F). However, the average intensity of individual clusters labeled with α-bungarotoxin (α-BTX) conjugated Alexa Fluor555 in Rac1-G12V myotubes was only half of that observed in control myotubes (Fig. 1G), suggesting a reduced AChR density. The average cluster area was not significantly changed, although very large clusters (>300 µm^2)

Journal of Cell Science (2018) 131, jcs215251. doi:10.1242/jcs.215251

were occasionally observed in Rac1-G12V myotubes (Fig. 1H). Together, these findings suggest that Rac1 is normally inhibited in mature myotubes, and that constitutive activation of Rac1 leads to elevation of actin polymerization at the myotube surface, as well as to excessive myotube fusion and disruption of AChR clustering. Because the dramatic change of AChR clusters is possibly a consequence of the myotube fusion instead of a direct regulation by Rac1 G12V, we only used Rac1-WT for activation of Rac1 in our subsequent studies of AChR clustering.

Rac1 is transiently activated at the initial stage of AChR clustering and rarely colocalized with AChR clusters

By adding agrin to C2C12 myotubes for different durations, we obtained a time-course pattern of AChR clustering. The first 2 h of agrin treatment appeared to be the initial stage of AChR clustering, as there was a high number of AChR microclusters (<5 μm^2) and a low number of full-sized clusters (≥5 μm^2; Fig. 2A,B). From 2–8 h of agrin treatment, the number of microclusters decreased by >50%, concomitantly with the dramatic 5-fold increase of full-sized clusters (Fig. 2A,B). The numbers of both full-sized clusters and microclusters remained relatively unchanged between 8 and 16 h (Fig. 2A,B), suggesting that agrin-induced AChR clustering reaches a maximum at 8 h, remaining stable afterwards. Interestingly, agrin induced a rapid and transient activation of Rac1, which peaked at 15 min and decreased to almost basal level at 60 min (Fig. 2C). This is consistent with previous reports (Linnoila et al., 2008; Weston et al., 2003), suggesting that Rac1 is only transiently activated at the initial stage of AChR clustering. To study the cocalization of active Rac1 relative to AChR clusters, we transfected myotubes with mRNAs of Rac1-WT or Rac-T17N, together with mRNA of YFP-PBD, followed by addition of agrin for 1.5 h. Rac1-WT, indeed, increased the number of active Rac1 clusters, whereas Rac1-T17N diminished active Rac1 clusters (Fig. 2D). Surprisingly, active Rac1 clusters were infrequently detected on the myotube surface or adjacent to AChR clusters, but rarely colocalized with AChR clusters (Fig. 2D). These observations suggest that Rac1 activation is associated with the dynamics of AChRs, such as AChR addition, movement or dispersal.

Initial formation of AChR clusters requires Rac1 activation

We first studied whether changes of Rac1 activity affect different stages of agrin-induced AChR cluster formation. Rac1-WT or T17N mRNA was transfected into myotubes, and agrin was added for 1.5 h or 8 h to induce initial and maximal clustering, respectively (Fig. 3A). Rac1-WT significantly increased the initial formation of microclusters (Fig. 3B,C), but Rac1-T17N inhibited the initial formation of both microclusters and full-sized clusters (Fig. 3B–E). When agrin was added for 8 h, Rac1-WT still increased microclusters, but both Rac1-WT and Rac1-T17N reduced the number of full-sized AChR clusters (Fig. 3F–I). These results suggest that, although Rac1 activation is required for the initial formation of AChR clusters, its prolonged activation prevents normal formation of full-sized clusters.

Stabilization of AChR clusters depends on Rac1 inhibition

As Rac1 is only transiently activated upon treatment with agrin, we introduced Rac1-WT and Rac1-T17N into myotubes after the initial phase of AChR clustering, i.e. transfection was performed after 1 h of agrin treatment when Rac1 activity had returned to basal levels (Fig. S3A). Interestingly, inhibition of Rac1 had almost no effect on AChR clustering (Fig. S3B–E). Activation of Rac1, however, decreased the number of AChR full-sized clusters but increased those of microclusters (Fig. S3B–E). This result is consistent with our previous observations that prolonged activation of Rac1 after the

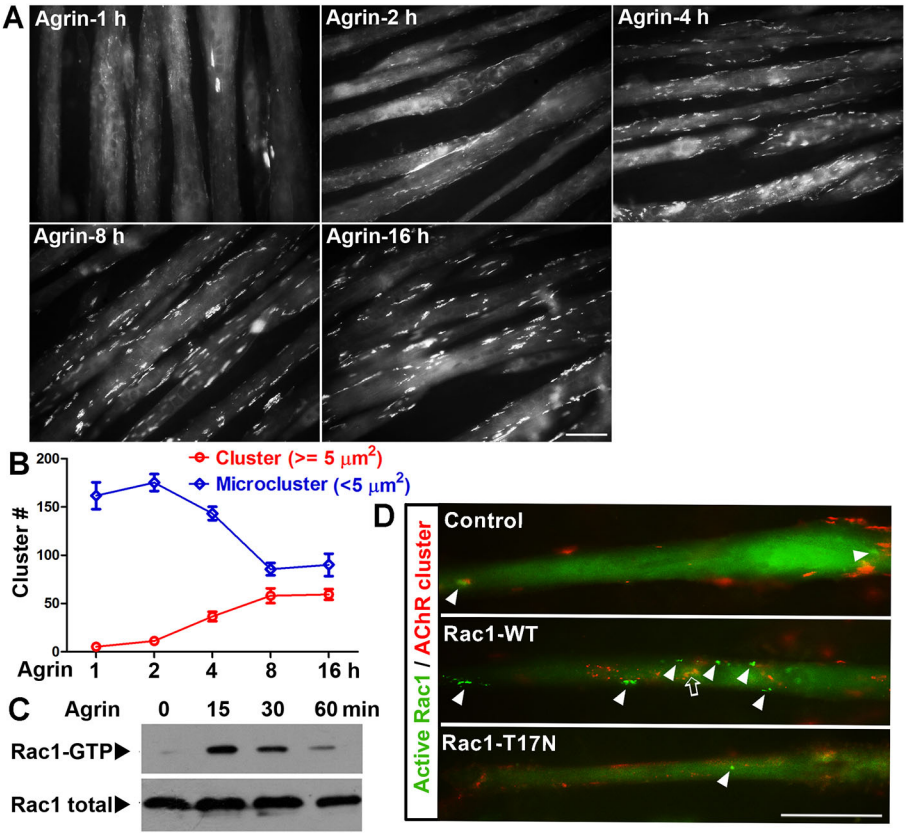

Fig. 2. Patterns and localization of activated Rac1 during AChR clustering. (A) C2C12 myotubes were treated with agrin for 1, 2, 4, 8 or 16 h, AChR clusters were stained by Alexa Fluor555-conjugated α-BTX. Scale bar: 50 μm. (B) Quantification analysis of AChR cluster (≥5 μm^2) and microcluster (<5 μm^2) numbers. (C) Agrin induces transient activation of Rac1. C2C12 myotubes were treated with agrin for 0–60 min, active Rac1 was pulled down by GST fused to PBD. (D) Myotubes were transfected with YFP-PBD mRNA together with Rac1-WT or T17N mRNA. Myotubes were fixed after they had been treated for 1.5 h with agrin. AChR clusters were stained with Alexa Fluor555-conjugated α-BTX. Arrowheads indicate clusters of activated Rac1 (green fluorescence of YFP-PBD that did not colocalize with AChR clusters), arrow indicates clusters of activated Rac1 colocalized with AChR clusters. Scale bar: 20 μm.

Journal of Cell Science (2018) 131, jcs215251. doi:10.1242/jcs.215251

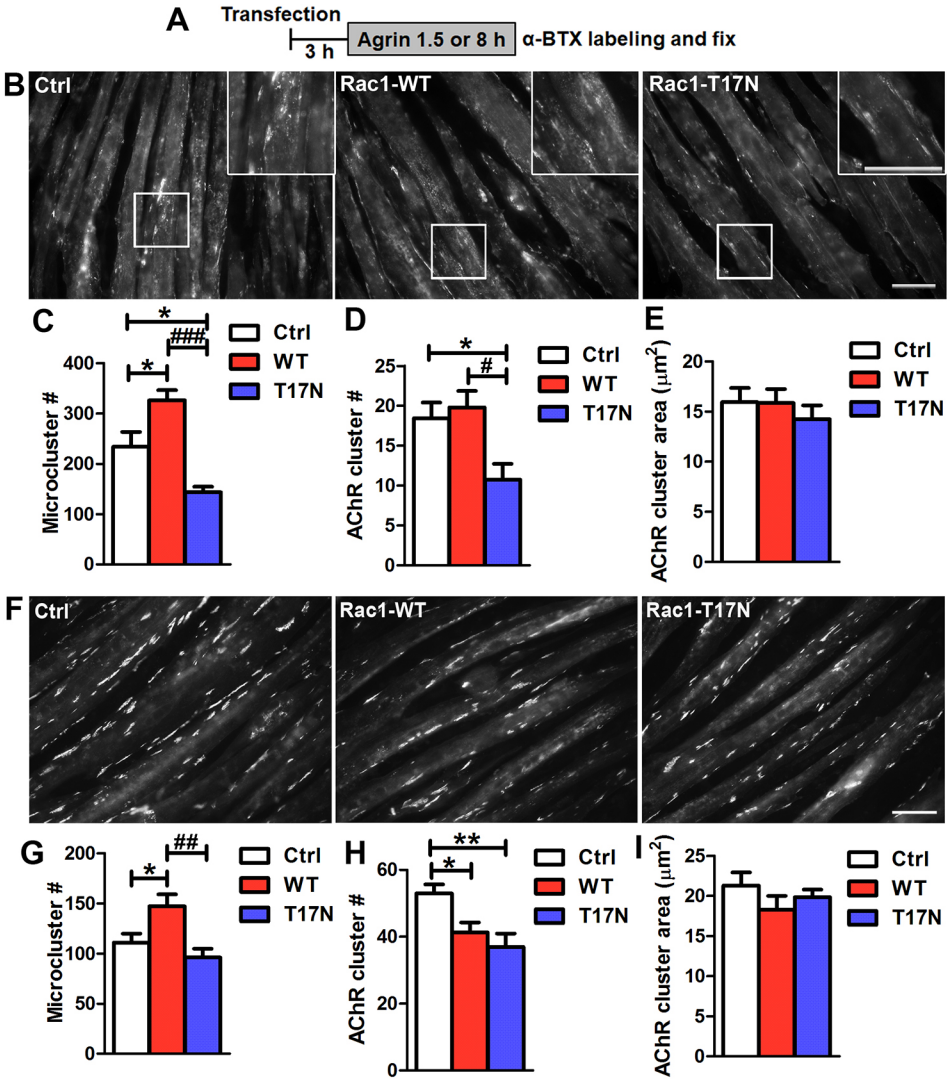

Fig. 3. Initial formation of AChR clusters requires Rac1 activation. (A) Schematic showing the examination of AChR clustering induced by treatment with agrin for 1.5 or 8 h, followed by labeling with Alexa Fluor-conjugated α-BTX. (B) Representative images showing AChR clusters at 1.5 h. Insets (top right corner) are magnifications of boxed areas showing small clusters and microclusters. (C) Number of AChR microclusters (<5 μm^2). **P*<0.05, Rac1-WT (WT) or Rac1-T17N (T17N) vs control (Ctrl); ###*P*<0.001, T17N vs WT. (D) Numbers of AChR clusters (≥5 μm^2). **P*<0.05, T17N vs Ctrl; #*P*<0.05, T17N vs WT. (E) Area of AChR clusters. (F) Representative images showing AChR clusters after 8 h of treatment with agrin. (G–I) Quantification of numbers of AChR microclusters (G), number of clusters (H) and cluster area (I). **P*<0.05, ***P*<0.01, WT or T17N vs Ctrl; ##*P*<0.01, T17N vs WT. All data are presented as mean±s.e.m. from at least three independent experiments. Statistical analysis was subjected to one-way ANOVA with Bonferroni multiple comparison test. All scale bars: 50 μm.

initial phase of AChR clustering impairs the formation of full-sized clusters. We then studied how alterations in Rac1 activity affect AChR stability. Myotubes were treated with agrin for 8 h, and AChR clusters were labeled with Alexa Fluor555-conjugated α-BTX. Rac1-WT or Rac1-T17N was then introduced to myotubes to study the dispersal of these 'pre-existing' AChR clusters (Fig. 4A). Notably, Rac1 activation caused accelerated removal of AChR clusters, indicated by the reduced number of full-sized clusters (Fig. 4B–D). We also quantified larger size (>20 μm^2) full-sized clusters and found that Rac1 activation decreased the area of these clusters (Fig. 4E). Rac1-T17N, however, caused more clusters of all sizes to be retained after agrin removal (Fig. 4B–E). Moreover, we labeled pre-existing clusters with a saturating dose of Alexa Fluor555-conjugated α-BTX. Unbound α-BTX was then washed off and the myotubes were re-incubated with agrin for another 12 h, followed by a second incubation with Alexa Fluor488-conjugated α-BTX (Fig. 4F). As α-BTX binds to AChRs in a relatively irreversible fashion, this two-round labeling method can be used to distinguish between pre-existing and newly formed clusters (Fig. S4) (Kummer et al., 2004). On the one hand, we observed that inhibition of Rac1 had no effect on pre-existing clusters but significantly reduced newly formed clusters (Fig. 4G–J). On the other hand, Rac1 activation decreased the number of pre-existing clusters but increased that of newly formed microclusters (Fig. 4G–J). Consistently, after Rac1 activation, the total cluster area was composed of fewer pre-existing clusters and more newly formed clusters (Fig. 4K). Together, these results suggest that Rac1 inhibition is important for the stabilization of pre-existing clusters, whereas Rac1 activation contributes to the dispersal and turnover of AChR clusters.

Pak1 mediates myotube fusion and destabilization of AChR clusters induced by Rac1 activation

Pak1, one of the most-studied downstream effectors of Rac1, has been suggested to be involved in the regulation of myotube formation and AChR clustering (Joseph et al., 2017; Luo et al., 2002). We found that Pak1 activity, indicated by its phosphorylation at Ser199 and Ser204, is tightly correlated with Rac1 activity (Fig. 5A). We then asked whether Rac1-induced myotube fusion and AChR cluster dispersal were mediated by Pak1. Indeed, the dominant-negative K298R mutation of Pak1 (Pak1-DN), which blocks Pak1 activity, markedly reversed the myotube fusion defects caused by Rac1-G12V (Fig. 5B,C). Pharmacological inhibition of actin polymerization with latrunculin A also inhibited Rac1-G12V-induced myotube fusion (Fig. 5D,E), suggesting that myotube fusion caused by Rac1 activation is mediated by Pak1 activation and actin polymerization. However, expression of Pak1-WT or of the constitutively active T422E Pak1 mutant (Pak1-CA) did not induce myotube fusion (Fig. S5), suggesting the involvement of other Rac1 effectors in this process.

Journal of Cell Science (2018) 131, jcs215251. doi:10.1242/jcs.215251

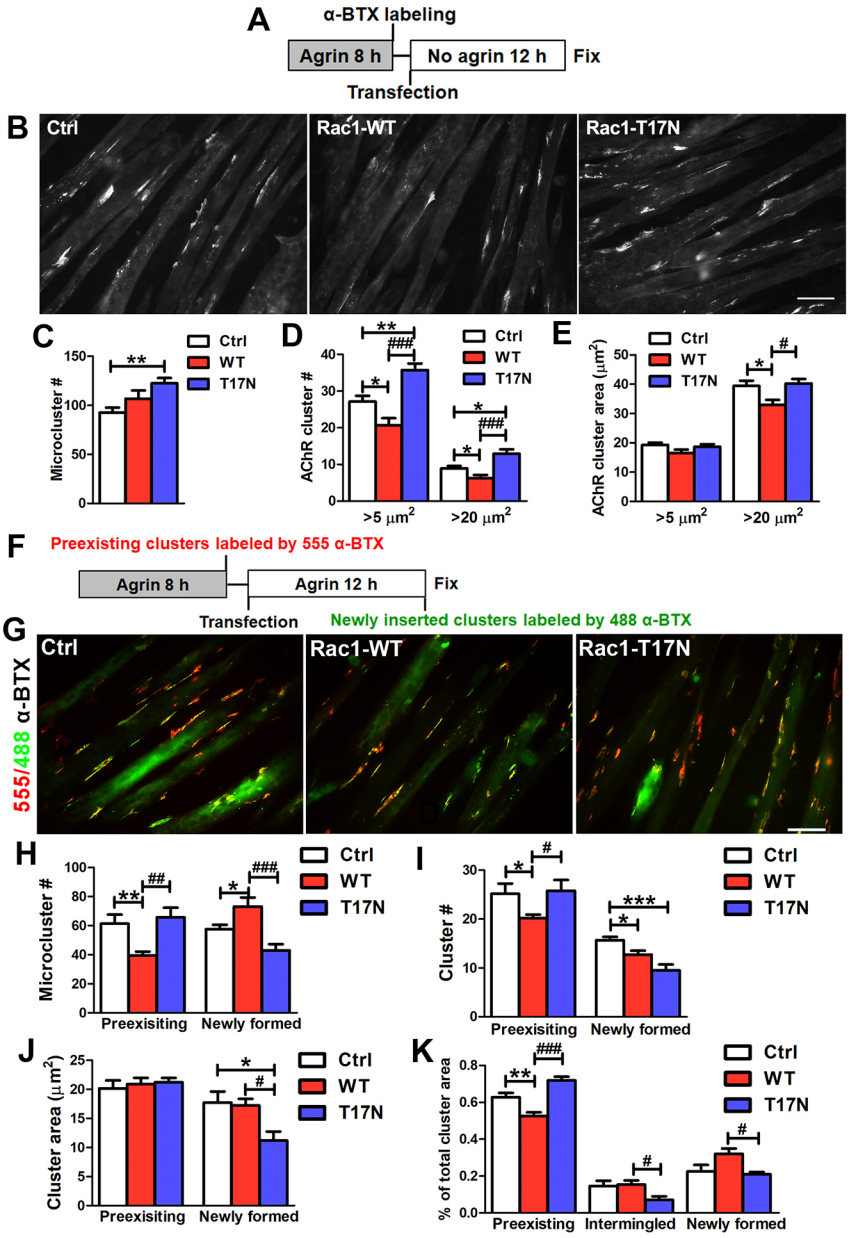

Fig. 4. Stabilization of AChR clusters depends on Rac1 inhibition. (A) Schematic showing the manipulation of Rac1 activity at the AChR cluster dispersal phase (treatment with agrin for 8 h, followed by no treatment for 12 h), followed by labeling with Alexa Fluor-conjugated α-BTX. (B) Rac1 activation accelerates AChR cluster dispersal. (C–E) Quantification of AChR microcluster number (C), cluster number (D) and cluster area (E). **P*<0.05, ***P*<0.01, Rac1-WT (WT) or Rac1-T17N (T17N) vs control (Ctrl); $^{\#}P$<0.05, $^{\#\#\#}P$<0.001, Rac1-T17N vs WT. (F) Schematic showing the examination of Rac1 activity on both pre-existing and newly formed clusters (treatment with agrin for 8 h, followed by no treatment for 12 h), followed by labeling with Alexa Fluor555-conjugated α-BTX. (G) Representative images showing pre-existing clusters labeled with Alexa Fluor555-conjugated α-BTX, and newly formed clusters labeled with Alexa Fluor488-conjugated α-BTX. (H,I) For each population of pre-existing or newly formed clusters, AChR microcluster number (H), cluster number (I) and cluster area (J) were quantified. (K) Quantification of pre-existing, newly formed and intermingled (containing both pre-existing and newly formed) clusters in percent. **P*<0.05, ****P*<0.001, Rac1-WT or T17N vs Ctrl; $^{\#}P$<0.05, $^{\#\#}P$<0.01, $^{\#\#\#}P$<0.001, Rac1-T17N vs WT. All data are presented as mean±s.e.m. from at least three independent experiments. Statistical analysis was subjected to one-way ANOVA with Bonferroni multiple comparison test. All scale bars: 50 μm.

Blocking the activation of the Arp2/3 complex – a downstream effector of Rac1 – by Wiskostatin failed to inhibit myotube fusion (Fig. 5D,E). To study the involvement of Pak1 in Rac1-mediated dispersal of pre-existing AChR clusters, we co-transfected Rac1-WT and Pak1-DN into myotubes after agrin had been added for 8 h and removed. Pak1 inhibition, indeed, blocked Rac1-mediated AChR destabilization (Fig. 5F,G). Therefore, Rac1-induced myotube fusion and AChR destabilization are largely mediated by Pak1.

Several GEFs and GAPs that activate Rac1 participate in the regulation of AChR clustering

We have shown that, in mature myotubes, Rac1 is generally inhibited, but that it is transiently activated during the formation of AChR clusters. Moreover, Rac1 is activated occasionally on the myotube surface and surrounds AChR clusters. Therefore, a precise spatiotemporal regulation of Rac1 activity is required to control the normal development of myotubes and AChR clusters. However, so far it is unknown which Rac1 GEFs or GAPs participate in the regulation of AChR clustering. To this end, we selected several Rac1 GEFs and GAPs that are expressed in the skeletal muscle, including Tiam1, Tiam2, Kalirin, Trio, α-PIX (ARHGEF6), β-PIX (ARHGEF7), Dock1, Dock4, Dock7, Vav1, Vav2, α2-chimaerin (CHN1), β2-chimaerin (CHN2) and BCR. To target individual factors, siRNAs were designed, whose knockdown efficiency was confirmed by real-time quantitative RT-PCR to be >60% (Fig. S6). We transfected each siRNA into myotubes and added agrin to induce AChR clustering. Interestingly, knockdown of α2-chimaerin, BCR, Kalirin, Trio, β-PIX, Dock1 and Vav1 led to decreased AChR clustering, whereas knockdown of Vav2 promoted AChR clustering (Fig. 6A–C). These results indicate that Rac1 is cooperatively regulated by multiple GAPs and GEFs during agrin-induced clustering of AChR.

DISCUSSION

Our study showed that, although Rac1 activation is required for agrin-induced AChR cluster formation, persistent activation of Rac1 leads to destabilization of AChR clusters; and constitutive activation of Rac1 even causes myotube fusion. Both myotube fusion and

Journal of Cell Science (2018) 131, jcs215251. doi:10.1242/jcs.215251

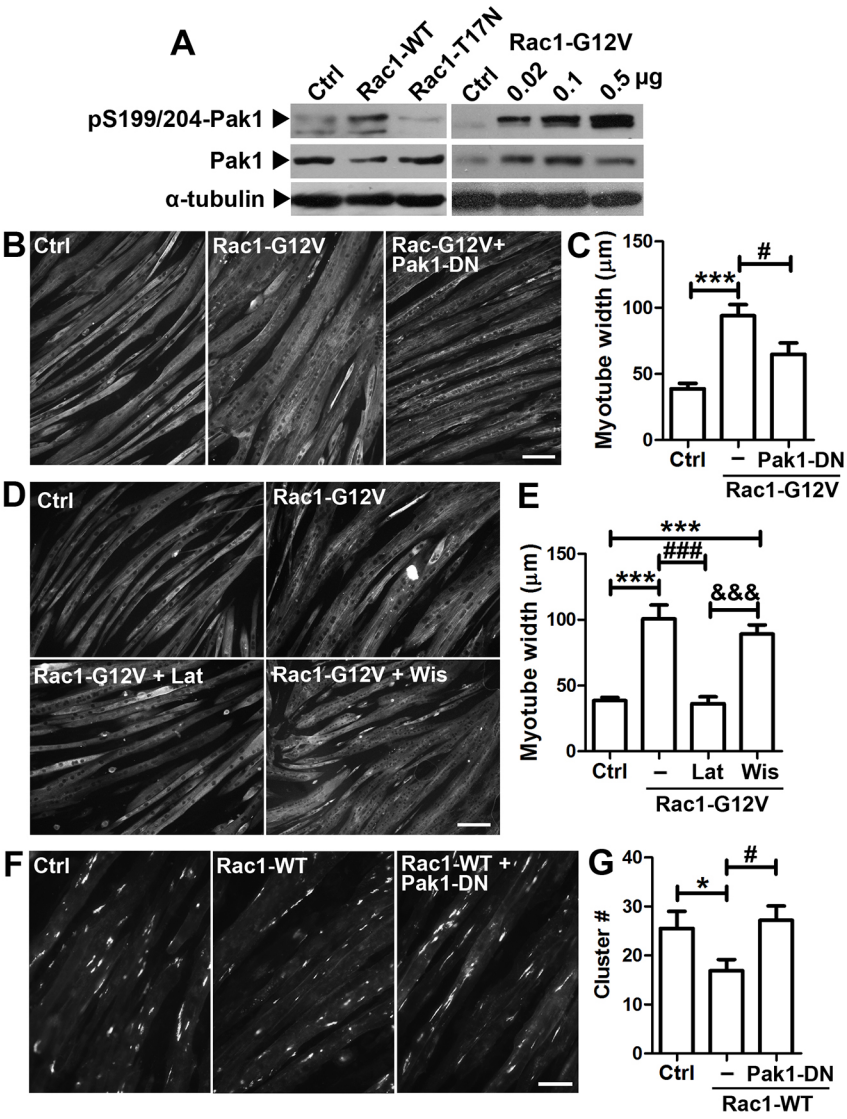

Fig. 5. Pak1 mediates Rac1 activity on myotube fusion and AChR cluster destabilization. (A) Levels of Pak1 phosphorylated at Ser199 and Ser204 (pS199/204-Pak1) were tightly correlated with the amount of active Rac1. Rac1-WT, Rac1-T17N or different amounts of Rac1-G12V were transfected into C2C12 myotubes; phosphorylation of Pak1 was examined by western blotting. (B) Inhibition of Pak1 reverses myotube fusion upon expression of Rac1-G12V. Rac1-G12V alone or together with Pak1-DN was transfected into myotubes, anti-MHC antibody was used to stain myotubes. (C) Quantification of myotube width. ***P<0.001, Rac-G12V vs Ctrl; $^{\#}P$<0.05, Rac1-G12V +Pak1-DN vs Rac1-G12V. (D) Myotube fusion induced by Rac1 hyperactivation was blocked upon addition of the actin polymerization inhibitor latrunculin A (Lat) or but not the Arp2/3 inhibitor. Myotubes were transfected with Rac1-G12V and treated with the actin polymerization inhibitor latrunculin A (Lat) or the Arp2/3 inhibitor Wiskostatin (Wis). (E) Quantification of myotube width. ***P<0.001, Rac1-G12V only or with Wis vs Ctrl; $^{\#\#\#}P$<0.001, G12V+Lat vs G12V; $^{\&\&\&}P$<0.001, Rac1-G12V+Wis vs G12V. (F) Pak1 inhibition restores stability of AChR clusters in Rac1-G12V-expressing myotubes. Myotubes were treated with agrin for 8 h, AChR clusters were labeled, and Rac1-G12V alone or together with Pak1-DN were transfected into myotubes. The myotubes were continuously cultured without agrin for 12 h. (G) Number of pre-existing AChR clusters was quantified. *P<0.05, Rac1-WT vs Ctrl; $^{\#}P$<0.05, Rac1-WT+Pak1-DN vs Rac1-WT. All data shown in this figure are presented as mean±s.e.m. from at least three independent experiments. Statistical analysis was subjected to one-way ANOVA with Bonferroni multiple comparison test. All scale bars: 50 μm.

AChR dispersal induced by Rac1 are dependent on Pak1 activation. The fact that inhibition of Rac1 hardly alters myotube morphology and AChR dispersal suggests that Rac1 activity is largely inhibited and not required for the terminal differentiation of myotubes and the maintenance of AChR clusters. Two Rac1 GAPs and Six Rac1 GEFs were found to be important for normal AChR clustering. Together, our study reveals that Rac1 is tightly regulated to ensure and control normal AChR clustering.

It has been shown previously that Rac1 activation at the onset of myoblast differentiation is required for myoblast fusion (Charrasse et al., 2007). Rac1 is involved in the organization of the lipid raft-containing fusion sites in myogenic cells (Mukai and Hashimoto, 2013). During the process of myotube formation, however, Rac1 activity is gradually decreased (Charrasse et al., 2007). Consistent with these findings, we have shown that inhibition of Rac1 in well-developed myotubes does not affect myotube morphology but that constitutive activation of Rac1 induces excessive myotube fusion. This suggests that, although activation of Rac1 mediates the initial myoblast fusion, it generally needs to be inhibited to shut down the fusion process once myotubes are properly formed. Nonetheless, Rac1 is not completely quiescent; and its active form is sparsely observed at the surface of mature myotubes. Therefore, mature muscle fibers may be still fusion-competent in order to remodel during muscle growth or regeneration. Here we demonstrated that Pak1 and actin polymerization are important to mediate the myotube fusion induced by Rac1. However, Pak1 alone is insufficient to cause myotube fusion. It would, therefore, be interesting to explore the involvement of other Rac1 effectors.

For the formation and maintenance of AChR clusters, the tight regulation of Rac1 activity is required. Rac1 activation, transiently induced by agrin, facilitates the initial phase of AChR cluster formation. We observed that Rac1-WT induces more microclusters shortly after treatment with agrin, whereas Rac1-T17N inhibits the formation of both microclusters and full-sized clusters (Fig. 7A,B). This is consistent with previous evidence that Rac1 activation leads to AChR microcluster formation (Weston et al., 2003, 2000). However, when examined in response to prolonged treatment with agrin (8 h), Rac1 activation decreases the number of full-size clusters and increases the number of microclusters, whereas Rac1 inhibition decreases the number of full-size clusters but does not trigger microcluster formation (Fig. 7A,B). This suggests that Rac1 activation promotes the initial formation of AChR clusters, but these clusters can be easily dispersed unless Rac1 is subsequently inhibited. Indeed, Rac1 activation accelerates the dispersal of pre-existing AChR clusters no matter whether agrin is present or not, and Rac1 activation also promotes replacement of pre-existing

Journal of Cell Science (2018) 131, jcs215251. doi:10.1242/jcs.215251

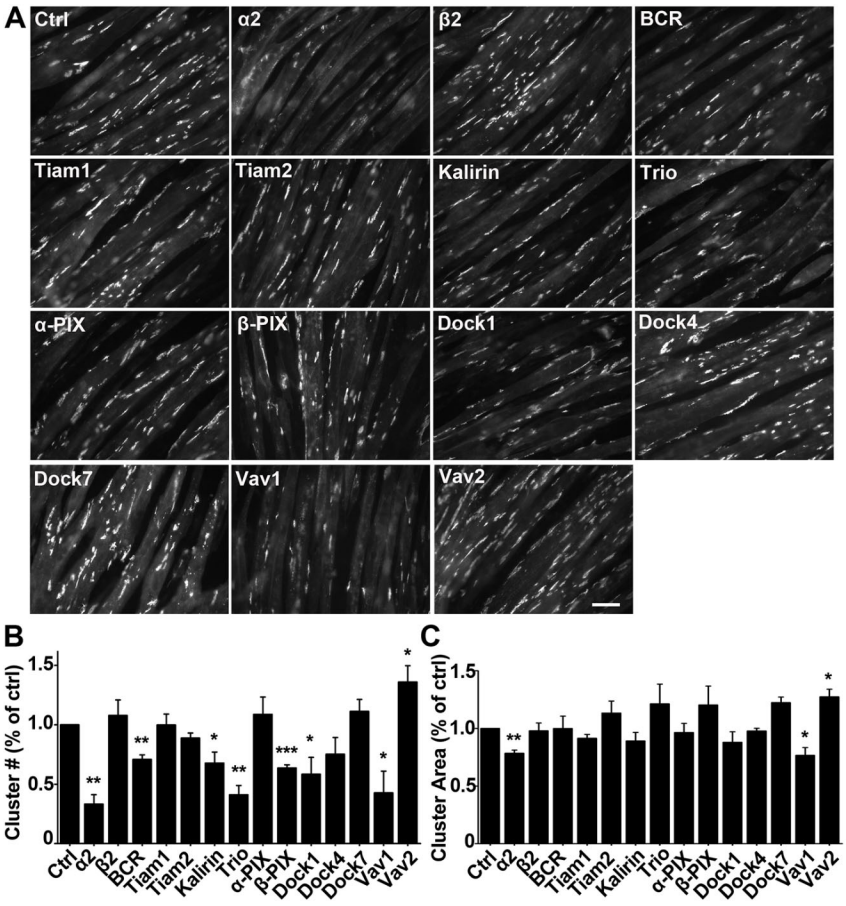

Fig. 6. Several Rac1 GEFs and Rac1 GAPs participate in the regulation of AChR clustering. (A) siRNAs of different Rac1 GEFs and Rac1 GAPs were transfected into C2C12 myotubes. Agrin was added for 8 h to induce AChR clustering. Scale bar: 50 µm. (B,C) Quantification of AChR cluster number (B) and area (C) after siRNA transfection of GEFs and GAPs normalized to those transfected with control siRNA (Ctrl). **P*<0.05, ***P*<0.01, ****P*<0.001, Student's *t*-test. Data are presented as mean±s.e.m. from at least three independent experiments.

clusters with newly formed ones. It has been shown previously that the endplate AChR clusters (i.e. AChR clusters at the postsynaptic muscle membrane of the neuromuscular junction) are relatively stable and have a long half-life, but recycling and intra-junctional migration of receptors are important processes that contribute to cluster dynamics (Akaaboune et al., 1999, 2002; Bruneau et al., 2005). In support with this notion, we found that active Rac1 rarely colocalizes with high-density AChR clusters; instead it is mainly present in close proximity to the clusters. Therefore, we propose that Rac1 activation, by promoting removal of pre-existing clusters and formation of new microclusters, regulates the dynamics and recycling of AChR clusters. The formation, refinement, maintenance and dispersal of AChR clusters may be tightly controlled by local activation or inhibition of Rac1.

Since Rac1 has to be accurately regulated to determine myotube development and AChR clustering, a complex mechanism for spatiotemporal Rac1 activity control must be involved. For this study, we screened 14 Rac1 GEFs and GAPs, and identified 8

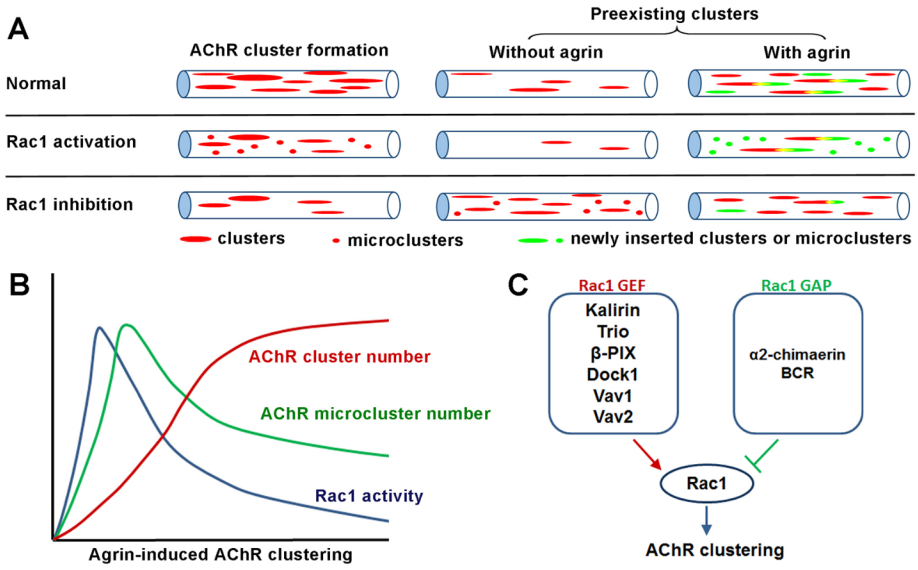

Fig. 7. A summary of the findings in this study. (A) Influences of Rac1 activation and inhibition on AChR cluster formation and stabilization at different stages. (B) A proposed pattern of changes of Rac1 activity, AChR microclusters and full-sized clusters during the course of agrin-induced AChR clustering. (C) Rac1 can be regulated by several GEFs and GAPs during AChR clustering.

that participate in AChR clustering, including the Rac1 GAPs α2-chimaerin and BCR, and the Rac1 GEFs Kalirin, Trio, β-PIX, Dock1, Vav1 and Vav2. To our knowledge, this is the first time that this set of Rac1 regulators has been reported to have functional roles in AChR clustering in skeletal muscle (Fig. 7C). Interestingly, Vav2 is the only Rac1 regulator that appears to have opposite roles compared with other identified regulators. Knockdown of Vav2 leads to the promotion of AChR clusters, whereas knockdown of either of the other 7 regulators always decreased the number of AChR clusters. Additional work regarding the expression and activation patterns of these Rac1 regulators is required to understand the action of each regulator and their cooperative modulation of Rac1 activity.

MATERIALS AND METHODS

Reagents, antibodies and constructs

Anti-Rac1 antibody was purchased from BD Biosciences (Cat# 610651; 1:2000 for western blotting), anti-MHC (anti-myosin heavy chain) antibody was from Millipore (Cat# 05-716; 1:4000 for immunocytochemistry), anti-α-tubulin antibody was from Sigma-Aldrich (Cat# T6074; 1:5000 for western blotting), antibodies against Pak1 (Cat# 2602; 1:2000 for western blotting) and phosphorylated Pak1 (at Ser199 and Ser204; Cat# 2605; 1:1000 for western blotting) were from Cell Signaling Technology. Alexa Fluor555 and Alexa Fluor488 conjugated to the neurotoxin α-BTX that labels AChRs were from Life Technologies. Recombinant rat C-terminal agrin was from R&D Systems. Latrunculin A and Wiskostatin were from Millipore. YFP-PBD plasmid was a gift from Joel Swanson (Addgene plasmid #11407) (Hoppe and Swanson, 2004). Mouse Rac1-WT, Rac1-T17N (dominant negative) and Rac1-G12V (constitutively active) plasmids have been described previously (IP et al., 2012; Xiao et al., 2013), and Rac1-Q61L (constitutively active) was generated by mutagenesis. Mouse Pak1 was cloned from mouse brain cDNA by RT-PCR and subcloned into pcDNA3.0 vector. Dominant negative Pak1-DN (K298R) and constitutively active Pak1-CA (T422E) mutants were generated by mutagenesis. The primers used for plasmid construction are shown in Table S1.

Cell culture and transfection

Mouse C2C12 myoblasts (ATCC) were cultured under 5% CO_2 and 95% air at 37°C as previously described (Shi et al., 2010a). Briefly, C2C12 myoblasts were maintained in Dulbecco's modified Eagle's medium (DMEM; Life Technologies) containing 20% fetal bovine serum (Life Technologies). Myotube differentiation was induced when myoblasts had grown to 100% confluency, growth medium was then switched to differentiation medium (DMEM supplemented with 2% horse serum, Life Technologies). Induction of AChR clustering was performed at day 3.5 of differentiation. For expression of YFP-PBD, Rac1, Pak1 or their mutant forms, we generated mRNAs by *in vitro* transcription using the mMESSAGE mMACHINE T7 Ultra Kit (Life Technologies). Respective mRNA (normally 0.5 µg, but 0.02–0.5 µg for Rac1-G12V and Rac1-Q61L) was transfected into C2C12 myotubes using Lipofectamine 2000 (Life Technologies). To study AChR formation and dispersal, mRNA was transfected 3 h before treatment with agrin, 1 h after agrin treatment or immediately after agrin had been removed, according to the experimental designs. For siRNA knockdown experiments, C2C12 myotubes were transfected with 40 nmol siRNA using Lipofectamine 2000 (Invitrogen) on day 2.5 of differentiation.

AChR clustering assay and myotube morphology analysis

For agrin-induced AChR clustering, C2C12 myotubes were treated with 10 ng/ml agrin for 1–16 h. AChR clusters were labeled in live myotubes using Alexa Fluor555-conjugated α-BTX. To examine the stability of AChR clusters, myotubes were treated with agrin for 8 h, and the AChR clusters were labeled by Alexa Fluor555-conjugated α-BTX as pre-existing clusters. Agrin was then washed off and myotubes were cultured in agrin-free medium for another 12 h. Alternatively, agrin was added again for another 12 h, and Alexa Fluor488-conjugated α-BTX was used to label newly formed AChR clusters. Myotubes were fixed using 4% paraformaldehyde at room temperature for 20–30 min. To analyze myotube fusion, anti-MHC antibody was used to stain the myotubes. F-actin was labeled by Rhodamine-phalloidin. Images of AChR clusters were captured by using a 40× objective and an ImagerA2 fluorescence microscope (Carl Zeiss AG). The myotube width, number and area of AChR clusters were quantified from 10 random fields using ImageJ software. Cluster areas of >5 µm^2 were counted as full-sized clusters, whereas those of <5 µm^2 were counted as microclusters. To analyze the fluorescence intensity of Alexa Fluor 555- and 488-conjugated α-BTX-labeled AChR clusters, Imaris 9.1.2 software was used. Briefly, a 2D rebuild surface that exactly draws out the clusters was created for each image by adjusting the values of Smooth and Threshold under the Surpass module. The average intensity, area and number of clusters were quantified.

Rac1 activity assay

Rac1 activity assay was carried out as described previously (Shi et al., 2007). Briefly, myotube proteins were harvested using a lysis buffer containing 50 mM Tris pH 7.2, 1% Triton X-100, 500 mM NaCl, 0.1% SDS, 0.5% sodium deoxycholate, 10 mM $MgCl_2$, 1 mM PMSF, 10 g/ml leupeptin and 10 g/ml aprotinin. GTP-Rac1 was pulled down by binding to glutathione-coupled agarose beads that had been conjugated to PBD-fused GST (GST-PBD) for 90 min at 4°C. The agarose beads were washed 3× with Tris buffer pH 7.2 (50 mM), containing 1% Triton X-100, 10 mM $MgCl_2$, 150 mM NaCl, 0.1 mM PMSF, 10 g/ml leupeptin and 10 g/ml aprotinin and then resuspended with 2× Laemmli sample buffer (Santa Cruz Biotechnology) and subjected to western blot analysis.

Knockdown of Rac1 GEFs and Rac GAPs in C2C12 myotubes

Four siRNAs were designed and synthesized for each gene by QIAGEN, the knockdown efficiencies were tested using quantitative RT-PCR. The sequences of the most effective siRNAs for individual genes are shown in Table S1.

Quantitative RT-PCR

Total RNA from C2C12 myotubes was isolated by using the RNAiso Plus kit (TaKaRa) following the manufacturer's suggested procedure. RT-PCR was performed as previously reported (Liao et al., 2018; Xiang et al., 2016). In brief, reverse transcription was performed to obtain cDNA products using M-MLV reverse transcriptase (Promega) and oligo(dT) primers. cDNAs were then mixed with iQ SYBR® Green (Bio-Rad) and qPCR was performed using a LightCycler 480 (Roche). Each PCR reaction was performed in triplicates and the GAPDH gene was used as an internal standard. The primers used for RT-PCR are shown in Table S1.

Statistical analysis

Data were presented as mean±standard error of mean (±s.e.m.) from at least three independent experiments, and analyzed by using GraphPad Prism 5 software. Statistically significant differences between two groups were analyzed by Student's *t*-test. Significant differences between multiple groups were determined by one-way ANOVA followed by Bonferroni Multiple Comparison Test.

Acknowledgements

We thank Dr Yuewen Chen and Miss Yumei Liao for their excellent technical assistance. We also thank Dr Yibo Qu, Dr Lisheng Peng, and Miss Xiaoxiao Li for sharing reagents. This work was supported in part by the National Natural Science Foundation of China [grant number 31471046]. L.S. is funded by The Academy of Medical Sciences Newton Advanced Fellowship in partnership with The Royal Society and The National Natural Science Foundation of China [UK/China grant numbers: NA160314/81761130084].

Competing interests

The authors declare no competing or financial interests.

Author contributions

Conceptualization: L.S.; Methodology: Y.B., Y.P., J.X., L.S.; Validation: Y.B., D.G., X.S., G.T., T.L.; Formal analysis: Y.B.; Investigation: Y.B., D.G., X.S., G.T., T.L., L.S.;

Data curation: Y.B.; Writing - original draft: Y.B., L.S.; Writing - review & editing: Y.B., L.S.; Supervision: L.S.; Project administration: L.S.; Funding acquisition: L.S.

Funding

This work was supported in part by the National Natural Science Foundation of China [grant number: 31471046]. L.S. is funded by The Academy of Medical Sciences Newton Advanced Fellowship in partnership with the Royal Society and the National Natural Science Foundation of China [UK/China grant numbers: NA160314 and 81761130084].

Supplementary information

Supplementary information available online at
http://jcs.biologists.org/lookup/doi/10.1242/jcs.215251.supplemental

References

Akaaboune, M., Culican, S. M., Turney, S. G. and Lichtman, J. W. (1999). Rapid and reversible effects of activity on acetylcholine receptor density at the neuromuscular junction in vivo. *Science* **286**, 503-507.

Akaaboune, M., Grady, R. M., Turney, S., Sanes, J. R. and Lichtman, J. W. (2002). Neurotransmitter receptor dynamics studied in vivo by reversible photo-unbinding of fluorescent ligands. *Neuron* **34**, 865-876.

Bai, Y., Xiang, X., Liang, C. and Shi, L. (2015). Regulating Rac in the nervous system: molecular function and disease implication of Rac GEFs and GAPs. *Biomed. Res. Int.* **2015**, 632450.

Basu, S., Sladecek, S., Martinez de la Peña y Valenzuela, I., Akaaboune, M., Smal, I., Martin, K., Galjart, N. and Brenner, H. R. (2015). CLASP2-dependent microtubule capture at the neuromuscular junction membrane requires LL5beta and actin for focal delivery of acetylcholine receptor vesicles. *Mol. Biol. Cell* **26**, 938-951.

Bruneau, E., Sutter, D., Hume, R. I. and Akaaboune, M. (2005). Identification of nicotinic acetylcholine receptor recycling and its role in maintaining receptor density at the neuromuscular junction in vivo. *J. Neurosci.* **25**, 9949-9959.

Charrasse, S., Comunale, F., Fortier, M., Portales-Casamar, E., Debant, A. and Gauthier-Rouvière, C. (2007). M-cadherin activates Rac1 GTPase through the Rho-GEF trio during myoblast fusion. *Mol. Biol. Cell* **18**, 1734-1743.

Dai, Z., Luo, X., Xie, H. and Peng, H. B. (2000). The actin-driven movement and formation of acetylcholine receptor clusters. *J. Cell Biol.* **150**, 1321-1334.

Dobbins, G. C., Zhang, B., Xiong, W. C. and Mei, L. (2006). The role of the cytoskeleton in neuromuscular junction formation. *J. Mol. Neurosci.* **30**, 115-118.

Gautam, M., Noakes, P. G., Mudd, J., Nichol, M., Chu, G. C., Sanes, J. R. and Merlie, J. P. (1995). Failure of postsynaptic specialization to develop at neuromuscular junctions of rapsyn-deficient mice. *Nature* **377**, 232–236.

Gawor, M. and Proszynski, T. J. (2018). The molecular cross talk of the dystrophin-glycoprotein complex. *Ann. N. Y. Acad. Sci.* **1412**, 62-72.

Henriquez, J. P., Webb, A., Bence, M., Bildsoe, H., Sahores, M., Hughes, S. M. and Salinas, P. C. (2008). Wnt signaling promotes AChR aggregation at the neuromuscular synapse in collaboration with agrin. *Proc. Natl. Acad. Sci. USA* **105**, 18812-18817.

Hoppe, A. D. and Swanson, J. A. (2004). Cdc42, Rac1, and Rac2 display distinct patterns of activation during phagocytosis. *Mol. Biol. Cell* **15**, 3509-3519.

Ip, J. P. K., Shi, L., Chen, Y., Itoh, Y., Fu, W.-Y., Betz, A., Yung, W.-H., Gotoh, Y., Fu, A. K. Y. and Ip, N. Y. (2012). alpha2-chimaerin controls neuronal migration and functioning of the cerebral cortex through CRMP-2. *Nat. Neurosci.* **15**, 39-47.

Jacobson, C., Côté, P. D., Rossi, S. G., Rotundo, R. L. and Carbonetto, S. (2001). The dystroglycan complex is necessary for stabilization of acetylcholine receptor clusters at neuromuscular junctions and formation of the synaptic basement membrane. *J. Cell Biol.* **152**, 435-450.

Joseph, G. A., Lu, M., Radu, M., Lee, J. K., Burden, S. J., Chernoff, J. and Krauss, R. S. (2017). Group I Paks promote skeletal myoblast differentiation in vivo and in vitro. *Mol. Cell. Biol.* **37**, e00222-16.

Kumari, S., Borroni, V., Chaudhry, A., Chanda, B., Massol, R., Mayor, S. and Barrantes, F. J. (2008). Nicotinic acetylcholine receptor is internalized via a Rac-dependent, dynamin-independent endocytic pathway. *J. Cell Biol.* **181**, 1179-1193.

Kummer, T. T., Misgeld, T., Lichtman, J. W. and Sanes, J. R. (2004). Nerve-independent formation of a topologically complex postsynaptic apparatus. *J. Cell Biol.* **164**, 1077-1087.

Lee, C. W., Han, J., Bamburg, J. R., Han, L., Lynn, R. and Zheng, J. Q. (2009). Regulation of acetylcholine receptor clustering by ADF/cofilin-directed vesicular trafficking. *Nat. Neurosci.* **12**, 848-856.

Liao, Y., Zhuang, X., Huang, X., Peng, Y., Ma, X., Huang, Z.-X., Liu, F., Xu, J., Wang, Y., Chen, W.-M. et al. (2018). A bivalent securinine compound SN3-L6 induces neuronal differentiation via translational upregulation of neurogenic transcription factors. *Front. Pharmacol.* **9**, 290.

Linnoila, J., Wang, Y., Yao, Y. and Wang, Z.-Z. (2008). A mammalian homolog of Drosophila tumorous imaginal discs, Tid1, mediates agrin signaling at the neuromuscular junction. *Neuron* **60**, 625-641.

Luo, Z. G., Wang, Q., Zhou, J. Z., Wang, J., Luo, Z., Liu, M., He, X., Wynshaw-Boris, A., Xiong, W. C., Lu, B. et al. (2002). Regulation of AChR clustering by Dishevelled interacting with MuSK and PAK1. *Neuron* **35**, 489-505.

Mukai, A. and Hashimoto, N. (2013). Regulation of pre-fusion events: recruitment of M-cadherin to microrafts organized at fusion-competent sites of myogenic cells. *BMC Cell Biol.* **14**, 37.

Nizhynska, V., Neumueller, R. and Herbst, R. (2007). Phosphoinositide 3-kinase acts through RAC and Cdc42 during agrin-induced acetylcholine receptor clustering. *Dev. Neurobiol.* **67**, 1047-1058.

Proszynski, T. J., Gingras, J., Valdez, G., Krzewski, K. and Sanes, J. R. (2009). Podosomes are present in a postsynaptic apparatus and participate in its maturation. *Proc. Natl. Acad. Sci. USA* **106**, 18373-18378.

Rossman, K. L., Der, C. J. and Sondek, J. (2005). GEF means go: turning on RHO GTPases with guanine nucleotide-exchange factors. *Nat. Rev. Mol. Cell Biol.* **6**, 167-180.

Sanes, J. R. and Lichtman, J. W. (1999). Development of the vertebrate neuromuscular junction. *Annu. Rev. Neurosci.* **22**, 389-442.

Sanes, J. R. and Lichtman, J. W. (2001). Induction, assembly, maturation and maintenance of a postsynaptic apparatus. *Nat. Rev. Neurosci.* **2**, 791-805.

Shi, L., Fu, W.-Y., Hung, K.-W., Porchetta, C., Hall, C., Fu, A. K. and Ip, N. Y. (2007). Alpha2-chimaerin interacts with EphA4 and regulates EphA4-dependent growth cone collapse. *Proc. Natl. Acad. Sci. USA* **104**, 16347-16352.

Shi, L., Butt, B., Ip, F. C. F., Dai, Y., Jiang, L., Yung, W.-H., Greenberg, M. E., Fu, A. K. Y. and Ip, N. Y. (2010a). Ephexin1 is required for structural maturation and neurotransmission at the neuromuscular junction. *Neuron* **65**, 204-216.

Shi, L., Fu, A. K. Y. and Ip, N. Y. (2010b). Multiple roles of the Rho GEF ephexin1 in synapse remodeling. *Commun. Integr. Biol.* **3**, 622-624.

Shi, L., Fu, A. K. Y. and Ip, N. Y. (2012). Molecular mechanisms underlying maturation and maintenance of the vertebrate neuromuscular junction. *Trends Neurosci.* **35**, 441-453.

Tcherkezian, J. and Lamarche-Vane, N. (2007). Current knowledge of the large RhoGAP family of proteins. *Biol. Cell* **99**, 67-86.

Weston, C., Yee, B., Hod, E. and Prives, J. (2000). Agrin-induced acetylcholine receptor clustering is mediated by the small guanosine triphosphatases Rac and Cdc42. *J. Cell Biol.* **150**, 205-212.

Weston, C., Gordon, C., Teressa, G., Hod, E., Ren, X.-D. and Prives, J. (2003). Cooperative regulation by Rac and Rho of agrin-induced acetylcholine receptor clustering in muscle cells. *J. Biol. Chem.* **278**, 6450-6455.

Wu, H., Xiong, W. C. and Mei, L. (2010). To build a synapse: signaling pathways in neuromuscular junction assembly. *Development* **137**, 1017-1033.

Xiang, X., Li, S., Zhuang, X. and Shi, L. (2016). Arhgef1 negatively regulates neurite outgrowth through activation of RhoA signaling pathways. *FEBS Lett.* **590**, 2940-2955.

Xiao, Y., Peng, Y., Wan, J., Tang, G., Chen, Y., Tang, J., Ye, W.-C., Ip, N. Y. and Shi, L. (2013). The atypical guanine nucleotide exchange factor Dock4 regulates neurite differentiation through modulation of Rac1 GTPase and actin dynamics. *J. Biol. Chem.* **288**, 20034-20045.